5 Tribological evaluation of castor oil–based greases

This chapter covers the tribological performance of castor oil–based grease with and without nanoadditives (MoS$_2$, MoS$_2$–ODT, GO, rGO, and GO–ODA). The greases were formulated with castor oil as a base oil and 12–lithium hydroxystearate metallic soap as a thickener. Tribological test results unveiled the role of nanoadditives on the lubrication performance of the castor oil–based grease.

5.1 Characterization of nanoadditives

In the present study, the synthesized MoS$_2$, MoS$_2$–ODT, GO, rGO, and GO–ODA nanosheets were used as additives in castor oil–based grease. The detailed chemical, structural, and morphological characterizations of nanoadditives were described in the previous **Sections 4.1 and 4.2**.

5.2 Physicochemical properties of castor grease

The synthesis procedure of castor oil–based lithium grease is reported in **Section 3.4**. The castor oil–based lithium grease without any nanoadditives is termed as *castor grease*. The castor grease samples were prepared having variable dosages (0.01–0.05 wt%) of MoS$_2$, MoS$_2$–ODT, GO, rGO, GO–ODA nanosheets and termed the prepared grease samples as *MoS$_2$ grease*, *MoS$_2$–ODT grease*, *GO grease*, *rGO grease*, and *GO–ODA grease*, respectively. The castor grease was used as a benchmark to compare the physicochemical and tribological properties of nanoadditives–blended grease samples.

The consistency and drop point of castor grease with and without nanoadditives were assessed as per ASTM D1403 and ASTM D566 standards, respectively. The test values of unworked and worked penetrations of castor grease samples with variable concentration nanoadditives are depicted in **Figure 5.1**. The worked penetration measurements were taken after shearing of grease via 60 double strokes. The worked penetration test result signifies NLGI grade 1 of the castor grease.
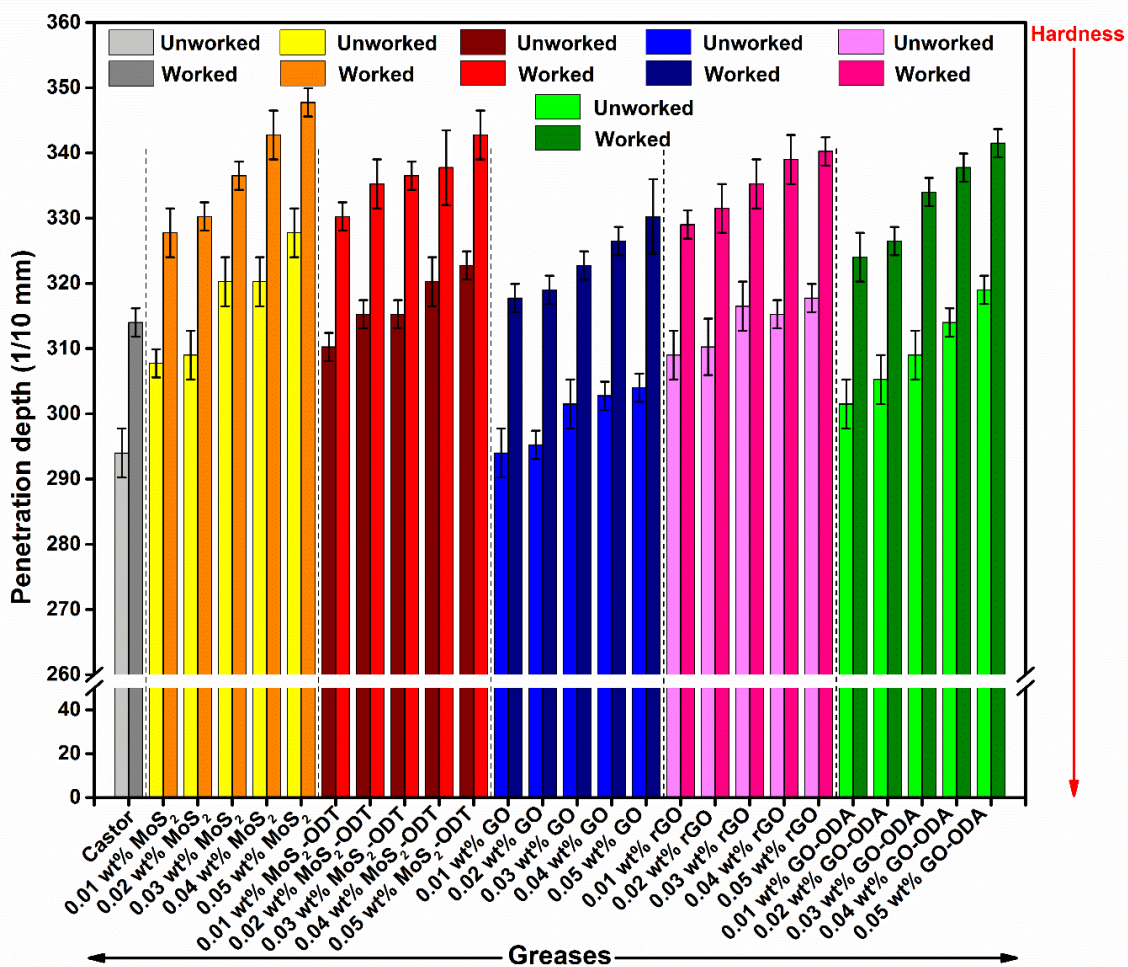

Figure 5.1: Variation in unworked and worked penetration depth of castor grease with and without nanoadditives

In the presence of MoS_2, MoS_2–ODT, GO, rGO, and GO–ODA nanoadditives in castor grease, the unworked penetration depth of castor grease samples is deteriorated. The worked penetration results suggest that the castor grease blended with MoS_2, MoS_2–ODT,

GO, rGO, and GO–ODA nanoadditives are semi–solid and can be classified as NLGI 1 grade. Furthermore, the variation in unworked and worked penetration shows the shear stability of the greases indicating that castor grease samples with and without nanoadditives have poor shear stability.
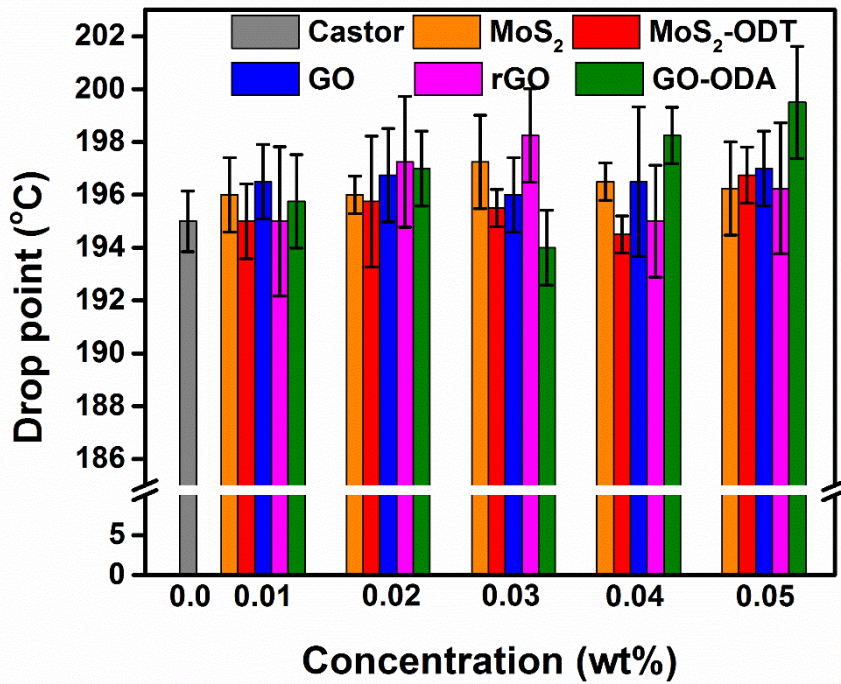

Figure 5.2: Variation in drop point of castor grease with and without nanoadditives

The drop point is a critical property that depends on the thickener used in grease formulation. It is a temperature at which the thickener fails to hold base oil inside the fibrous mesh of the thickener. This might be possible due to the melting of the thickener or the base oil in the influence of heat transforming so that thin capillary action and surface tension become insufficient to retain the base oil inside the fibrous mesh of the thickener. The change in drop point of castor grease with variable concentration of nanoadditives is shown in **Figure 5.2**. From the test results of a drop point, it can be observed that the presence of nanoadditives in castor grease within a given range was incapable of augmenting the drop point of castor grease.

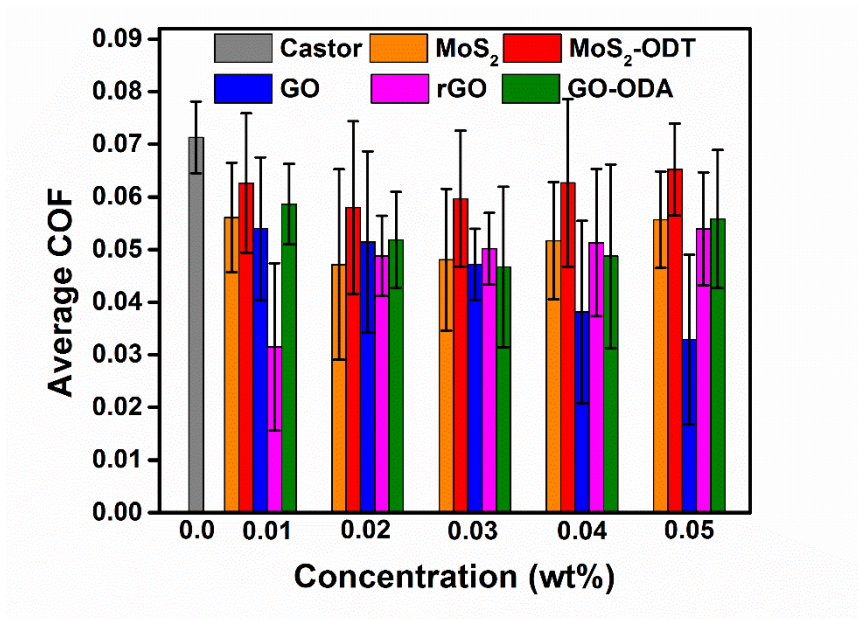## 5.3 Tribological performance of castor greases on four–ball tester

Figure 5.3: Variation in average COF with variable concentration of nanoadditives in castor grease. (Applied load: 392 N, test duration: 60 min)

The tribological behavior of castor grease was assessed in the presence of MoS_2, MoS_2–ODT, GO, rGO, and GO–ODA nanosheets using a four–ball tester as per ASTM D2266 standard. **Figure 5.3** shows the trend of average coefficient of friction (COF) with increasing concentration of nanoadditives in the castor grease. The castor grease without any nanoadditives displays high COF ($\mu = 0.071$) between the mating steel balls surfaces. The addition of MoS_2, MoS_2–ODT, GO, rGO, and GO–ODA nanosheets decreased the COF, and it was variable with their concentration in the castor grease. MoS_2 and MoS_2–ODT greases exhibited minimum friction at 0.02 wt%, which are 34% and 19% lower than that of castor grease, respectively. The 0.05 and 0.01 wt% doses of GO and rGO nanosheets in castor grease exhibited the maximum reduction in COF, i.e., 54% and 56%, respectively. The GO–ODA grease showed a maximum reduction in friction (35%) at 0.03 wt%. The friction results suggest that MoS_2, MoS_2–ODT, GO, rGO, and GO–ODA nanosheets in castor grease for a given concentration range have qualified as antifriction (AF) additives.
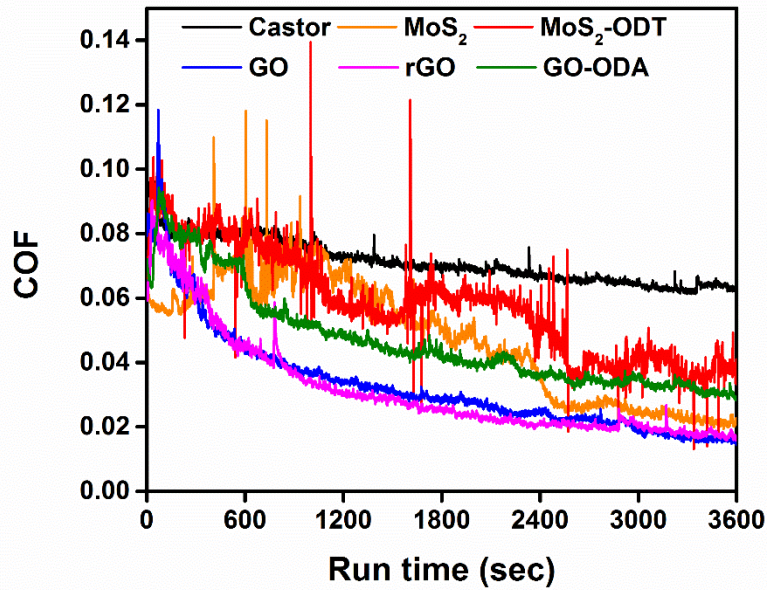
Figure 5.4: Variation in COF for castor grease with and without nanoadditives with run time. (Applied load: 392 N, test duration: 60 min)

Figure 5.4 shows the variation in COF with a function of time for castor grease with and without MoS_2 (0.02 wt%) and MoS_2–ODT (0.02 wt%), GO (0.05 wt%), rGO (0.01 wt%), and GO–ODA (0.03 wt%) nanosheets. The castor grease exhibited a higher COF throughout the running–in period. The smooth and stable friction profile of castor grease indicates that a stable tribo–film was established between tribo–pairs. The addition of MoS_2 and MoS_2–ODT nanosheets in castor grease significantly decreased the COF, but several undulations in the friction profile indicated that MoS_2 and MoS_2–ODT greases were unable to maintain the continuous tribo–film between the steel balls. It may be happening by stuck wear debris generated during the frictional contact (Gupta and Harsha, 2018a). Doping of GO, rGO, and GO–ODA nanosheets significantly decreased the COF and established a comparatively good quality of tribo–film between the interacting surfaces. It suggests a continuous supply of graphene–based nanomaterial between interacting surfaces, which furnished a protective tribo–film that prevented the direct contact of asperities.

Table 5.1: Energy saving with the use of MoS$_2$, MoS$_2$–ODT, GO, rGO, and GO–ODA nanoadditives in castor grease

Samples	Parameters	Concentration (wt%)					
		0.0	0.01	0.02	0.03	0.04	0.05
MoS$_2$ grease	Power consumption (MJ)	56.7	44.6	37.5	38.2	41.1	44.3
	% reduction in power consumption	—	21	34	33	28	22
MoS$_2$–ODT grease	Power consumption (MJ)	56.7	49.8	46.1	47.5	49.9	51.9
	% reduction in power consumption	—	12	19	16	12	9
GO grease	Power consumption (MJ)	56.7	42.9	40.9	37.6	30.4	26.2
	% reduction in power consumption	—	24	28	24	47	54
rGO grease	Power consumption (MJ)	56.7	25.1	38.8	39.9	40.8	42.9
	% reduction in power consumption	—	56	32	30	28	24
GO–ODA grease	Power consumption (MJ)	56.7	46.7	41.3	37.2	38.8	44.4
	% reduction in power consumption	—	18	27	35	32	22

Frictional energy losses in interacting surfaces are directly related to friction generated between tribo–contacts. A significant amount of energy is consumed in tribo–contacts to overcome the friction. The presence of nanoadditives in castor grease has reduced the friction and conserves the energy by decreasing the frictional losses. The amount of energy saved by castor grease in the presence of variable dosages of MoS$_2$, MoS$_2$–ODT, GO, rGO, and GO–ODA nanosheets are reported in **Table 5.1**. The castor grease consumed maximum energy (18.91 MJ) to overcome the frictional losses. The optimized dosage of MoS$_2$, MoS$_2$–ODT, GO, rGO, and GO–ODA saved energy by ~34%, ~19% ~54%, ~56%, and ~35%, respectively. Comparisons of energy–saving results reveal that the minute dosage of GO and rGO nanosheets in castor grease conserve the maximum energy. Moreover, the result

suggests that the addition of infinitesimal concentration of nanoadditives in the grease has a promising ability to conserve energy.
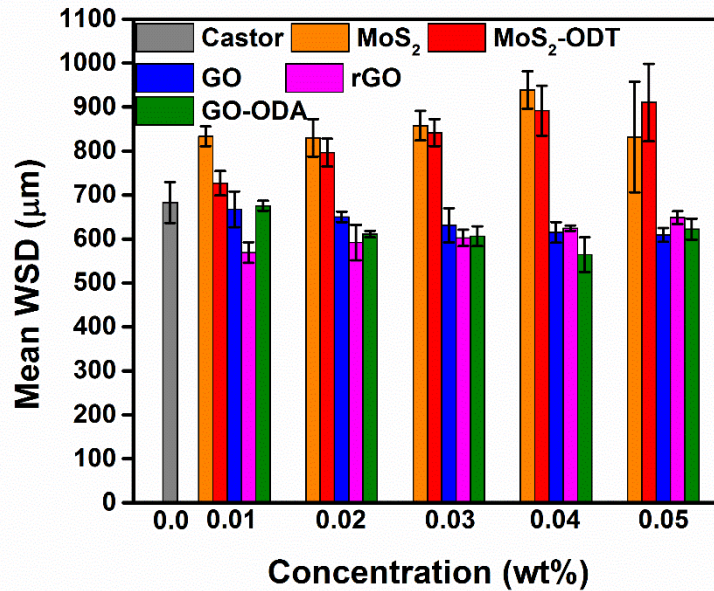

Figure 5.5: Variation in mean WSD with variable concentration of nanoadditives in castor grease. (Applied load: 392 N, test duration: 60 min)

The variation in wear scar diameter (WSD) for castor grease samples having variable dosages (0.01 to 0.05 wt%) of MoS_2, MoS_2–ODT, GO, rGO, and GO–ODA nanosheets is shown in **Figure 5.5**. The castor grease has developed a wear scar of 683 μm on the surface of steel balls. The addition of MoS_2 and MoS_2–ODT nanosheets in castor grease has enlarged the WSD gradually as the concentration of MoS_2 and MoS_2–ODT nanosheets increased. On the other hand, WSD has decreased gradually by incorporating GO and GO–ODA nanosheets in castor grease. The 0.01 wt% concentration of rGO nanosheets as an additive in castor grease showed a maximum decrement in WSD (~16%). The 0.05 wt% and 0.04 wt% concentrations of GO and GO–ODA nanosheets displayed a maximum reduction in WSD and were found to be ~10% and ~17%, respectively. Comparisons of antiwear (AW) results suggest that GO, rGO, and GO–ODA nanosheets in castor grease for the given concentration range have shown excellent AW performance, while for the

given concentration range, MoS$_2$ and MoS$_2$–ODT nanosheets are not compatible with castor grease as AW additive.
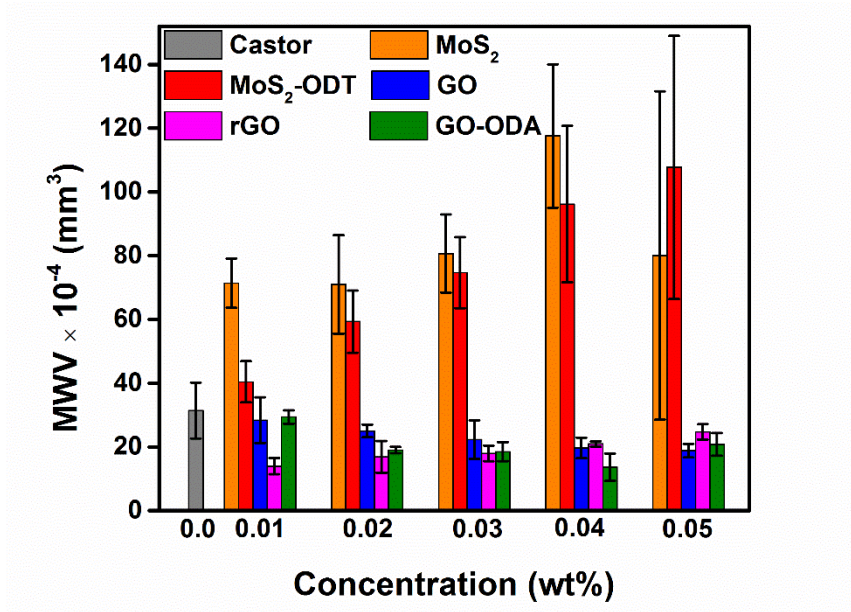

Figure 5.6: Variation in MWV with variable concentration of nanoadditives in castor grease. (Applied load: 392 N, test duration: 60 min)

The variations in mean wear volume (MWV) for castor grease samples with the variable concentration of MoS$_2$, MoS$_2$–ODT, GO, rGO, and GO–ODA nanosheets are shown in **Figure 5.6**. The MWV of castor grease in the presence of MoS$_2$ and MoS$_2$–ODT nanosheets increased gradually with the increasing concentration of MoS$_2$ and MoS$_2$–ODT nanosheets. The 0.04 wt% concentration of GO–ODA nanoadditives in castor grease exhibited a maximum reduction of ~56% in MWV. The 0.05 wt% of GO nanosheets furnished a maximum reduction of ~40% in MWV, whereas 0.01 wt% of rGO nanosheets exhibited a maximum reduction of ~55% in MWV than castor grease. The tribological results of castor grease blended with MoS$_2$, MoS$_2$–ODT, GO, rGO, and GO–ODA nanosheets revealed that graphene–based nanomaterials exhibit superior lubrication behavior than MoS$_2$–based nanomaterials.
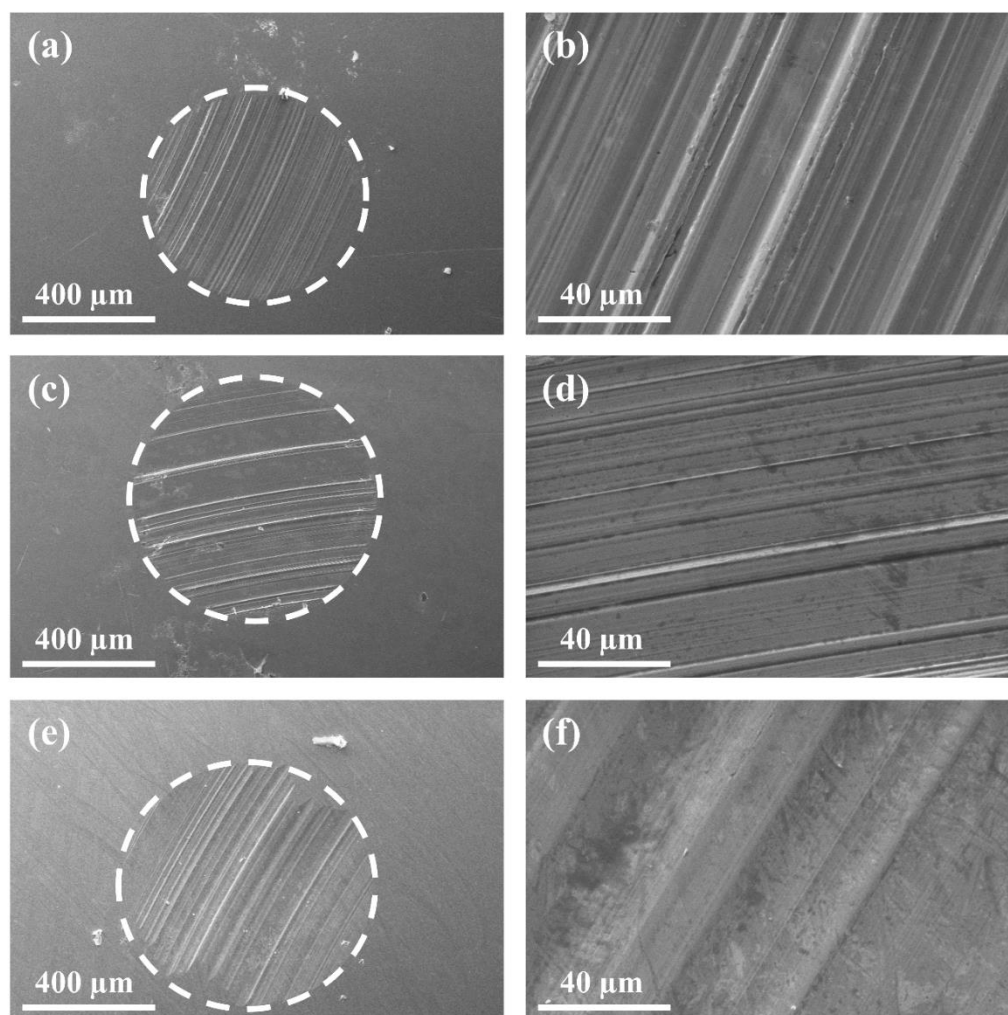
5.4   Study of worn surfaces

Figure 5.7: SEM images of worn surfaces of steel balls lubricated with (a–b) castor grease (c–d) 0.02 wt% MoS_2 nanosheets in grease (e–f) 0.01 wt% MoS_2–ODT nanosheets in grease. (Applied load: 392 N, test duration: 60 min)

Figure 5.7a shows the SEM micrographs and morphology of the worn surface of steel balls lubricated with castor grease. The deep furrows revealed the severity of wear and evidence for the plastic deformation. The scratches and furrows are distributed in large numbers and parallel to the sliding direction. These furrows are deep and rough. The high–resolution micrograph (**Figure 5.7b**) of the worn surface demonstrated that the well–defined furrows and typical features of abrasion wear. The number of furrows is fewer, smoother, and less deep in the worn surface when MoS_2 nanosheets are used as nanoadditives in castor grease

(**Figure 5.7c–d**). Similarly, the scratches marks are not seen in the presence of MoS_2–ODT nanosheets (**Figure 5.7e–f**).
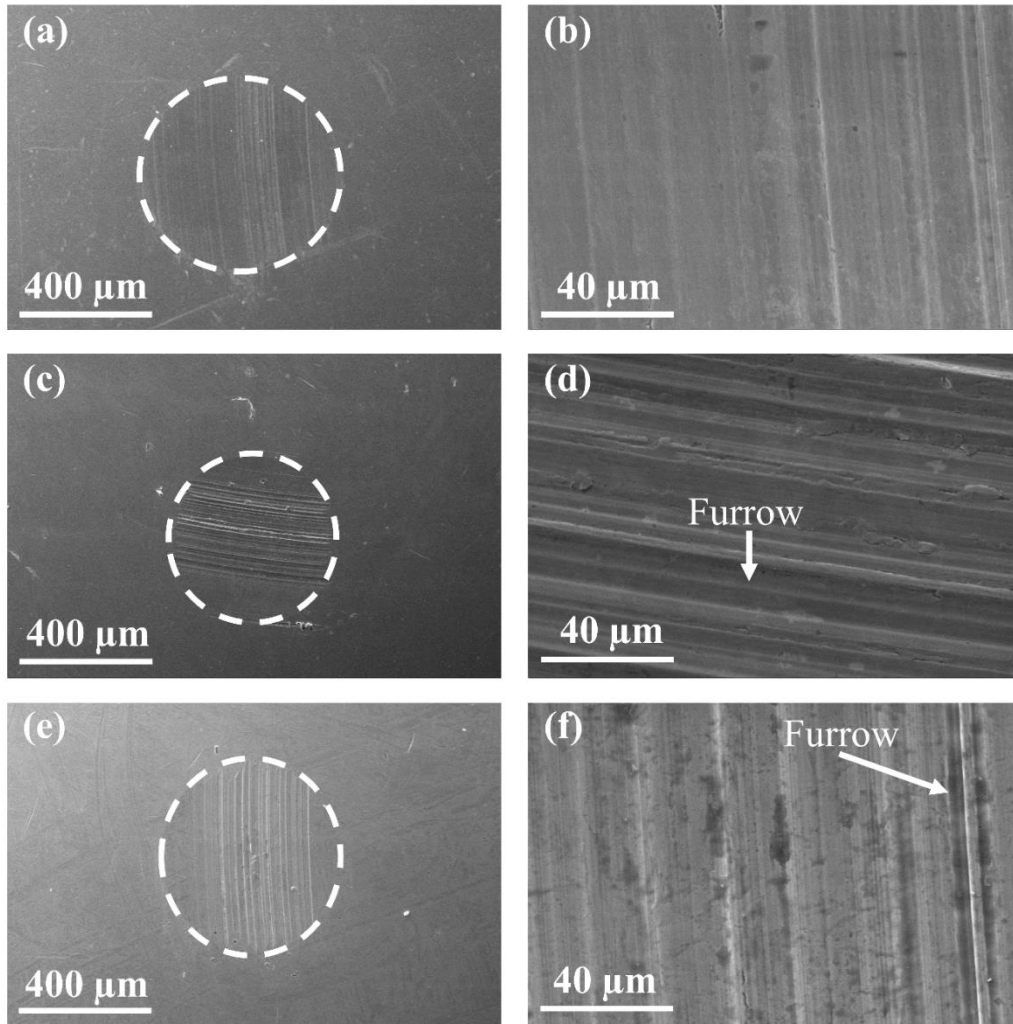

Figure 5.8: SEM images of worn surfaces of steel balls lubricated with (a–b) 0.05 wt% GO nanosheets in grease (c–d) 0.01 wt% rGO nanosheets in grease (e–f) 0.04 wt% GO–ODA nanosheets in grease. (Applied load: 392 N, test duration: 60 min)

Figure 5.8a–b shows the SEM micrographs and wear pattern of worn surface of steel ball lubricated with GO nanosheets as an additive in castor grease. The furrows and scratches are diminished in the presence of GO nanosheets. The number of furrows and their depth is reduced in the presence of rGO nanosheets (**Figure 5.8c–d**). Similarly, smoother and shallow furrows are observed when GO–ODA nanosheets were used as an additive (**Figure**

5.8e–f). Comparisons of SEM micrographs suggest that graphene–based nanoadditives significantly reduced the severity of wear and plastic damage of materials. The two–dimensional (2D) morphology of graphene–based materials allow them to enter the tribo–contact. These nanosheets could break under the Hertzian contact stress of ~3.4 GPa and generated small lateral sheets that maintained the uninterrupted supply of graphene nanosheets.
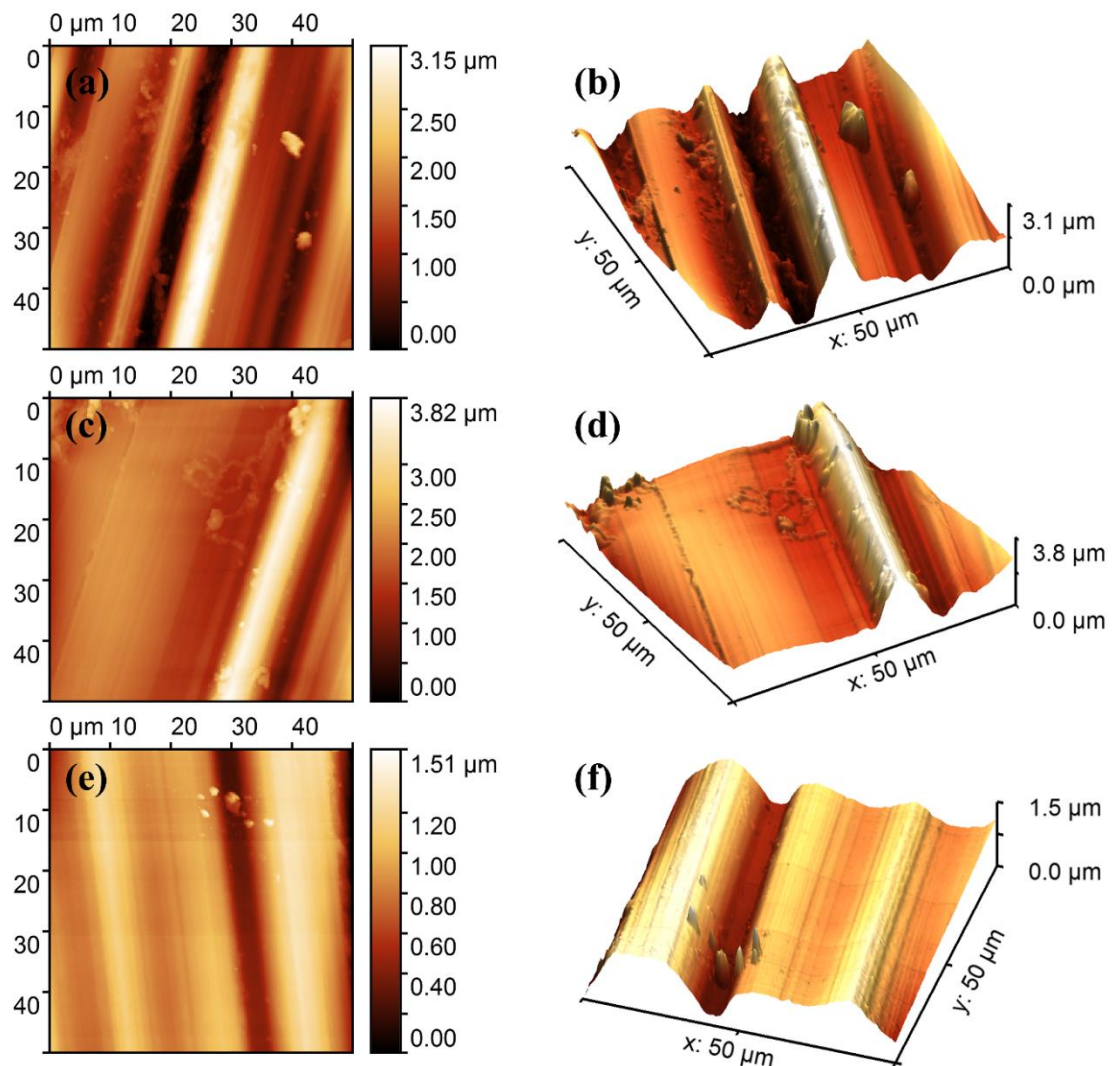

Figure 5.9: Topographic images of the worn surfaces of steel balls used in the tribo–tests in the presence of (a–b) castor grease, (c–d) 0.02 wt% MoS_2 nanosheets in grease (e–f) 0.01 wt% MoS_2–ODT nanosheets in grease. (Applied load: 392 N, test duration: 60 min)

The SPM images of worn surfaces were acquired for the quantitative estimation of roughness features. The topographic and corresponding three-dimensional (3D) images of worn surface lubricated with castor grease explicitly illustrate corrugated features and deep furrows (**Figure 5.9a–b**). The well–defined deep furrows are shown in the 3D image (**Figure 5.9b**) indicate the severity of wear with the plausibility of abrasion. The high stick–slip events were occurred due to intermittent contact between asperities. As a result, high adhesion–driven wear arisen and consequence high roughness was achieved. It validates the high friction and wear results of castor grease.

The topographic and 3D images of worn surface lubricated with MoS_2 blended castor grease are shown in **Figure 5.9c–d**. The presence of MoS_2 nanosheets has decreased the roughness and produced smoother surfaces than castor grease. Similarly, the surface roughness of worn surface lubricated with MoS_2–ODT–doped grease has reduced significantly and yielded a comparatively smoother surface (**Figure 5.9e–f**). The surface roughness of worn surfaces of the steel balls lubricated with various castor greases is presented in **Table 5.2**.

Table 5.2: Roughness of worn surfaces of the steel balls lubricated with various castor greases

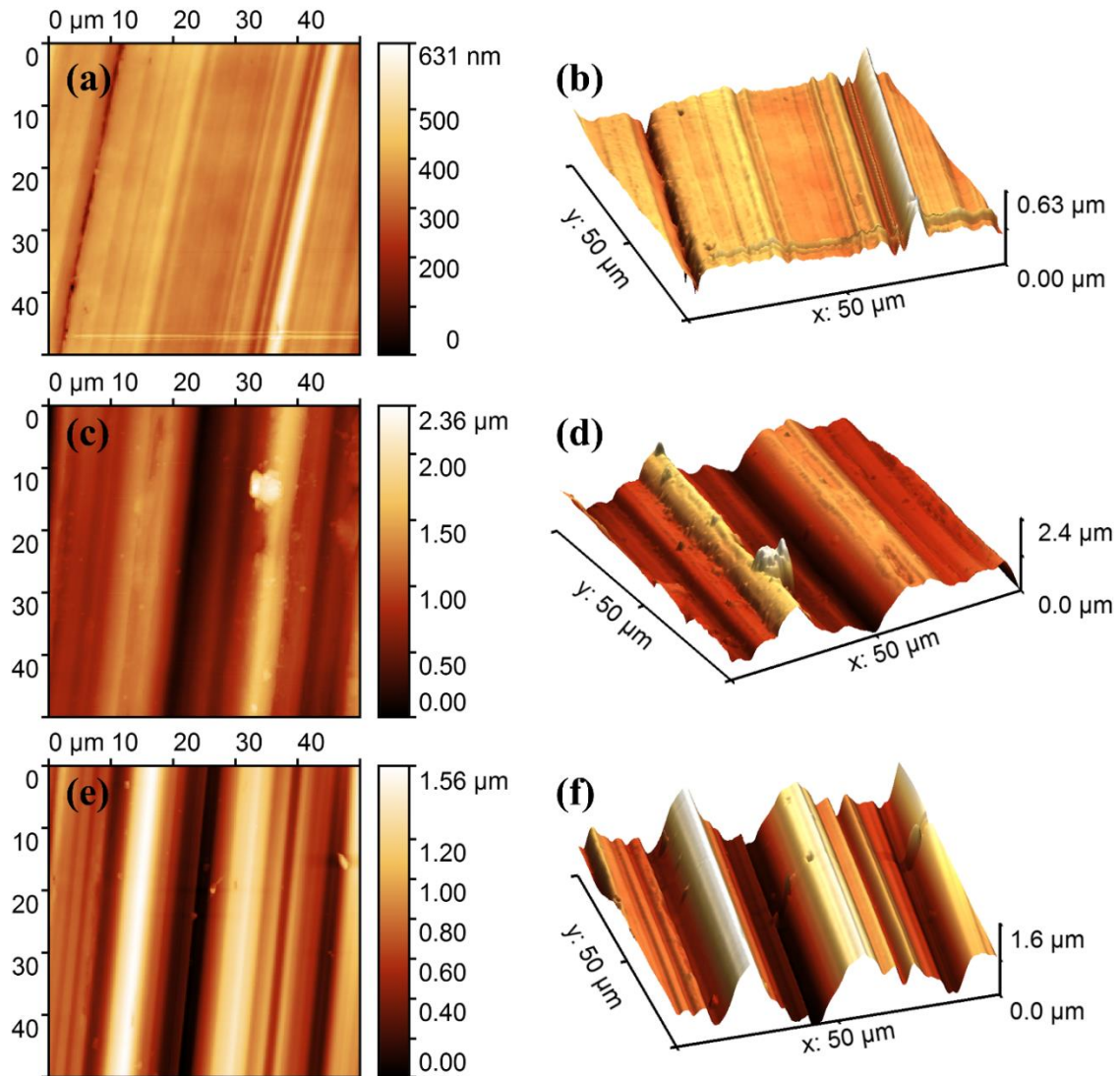| Samples	Surface roughness parameters			
	S_a, nm	S_q, nm	S_{sk}	S_{ku}
Castor grease	484	626	0.64	0.43
MoS_2 grease	418	573	0.88	1.26
MoS_2–ODT grease	182	241	0.71	0.46
GO grease	37	55	1.00	4.64
rGO grease	285	364	0.41	0.10
GO–ODA grease	294	366	0.21	− 0.60

Figure 5.10: Topographic images of the worn surfaces of steel balls used in the tribo–tests in the presence of (a–b) 0.05 wt% GO nanosheets in grease, (c–d) 0.01 wt% rGO nanosheets in grease (e–f) 0.04 wt% GO–ODA nanosheets in grease. (Applied load: 392 N, test duration: 60 min)

The topographic and 3D images of worn surface lubricated with GO, rGO, and GO–ODA nanosheets blended castor grease is shown in **Figure 5.10a–f**. The presence of graphene–based nanoadditives has lowered the peak–to–peak roughness and diminished the corrugated features. Further, the absence of adhesive wear suggested that graphene–based nanoadditives maintained a beneficial tribo–film at tribo–contacts, which prevented direct asperities to asperities interaction/contact. Comparisons of SPM results suggested that

graphene–based nanoadditives significantly reduced the surface roughness and improved AW property than MoS_2–based nanoadditives.
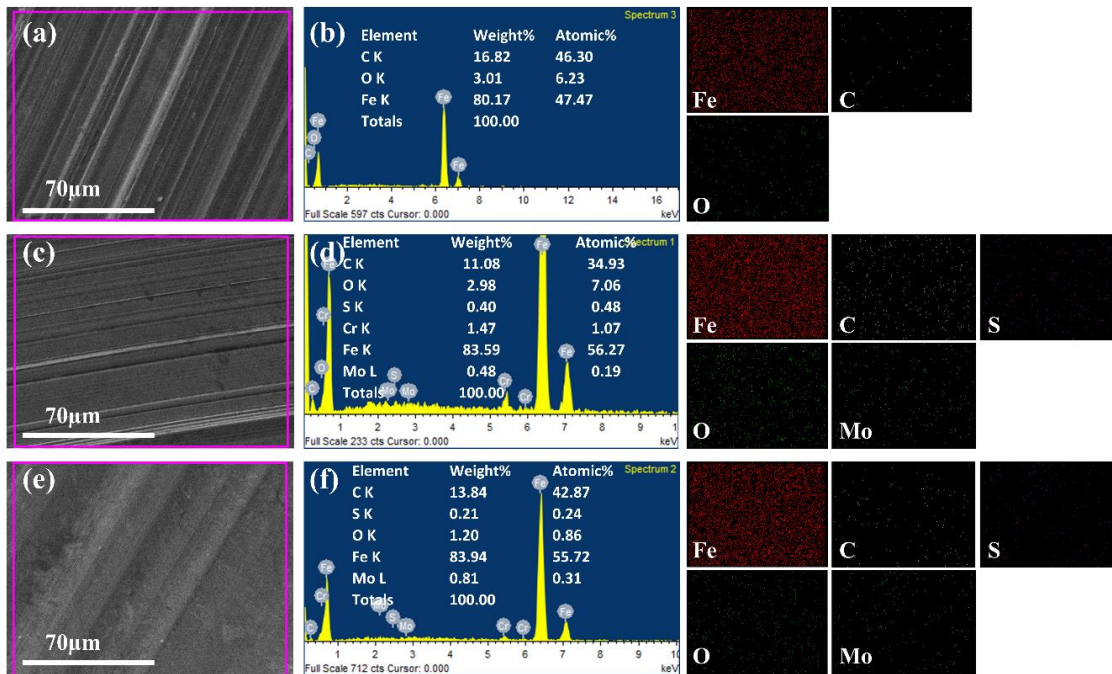

Figure 5.11: EDS spectra with elemental mapping of corresponding worn surfaces of (a–b) castor grease (c–d) 0.02 wt% MoS_2 nanosheets in grease (e–f) 0.01 wt% MoS_2–ODT nanosheets in grease. (Applied load: 392 N, test duration: 60 min)

The EDS analysis along with elemental mapping corresponding to worn surfaces was executed to understand the chemical nature and elemental distribution of nanoadditives on interacting surfaces. The EDS spectra of steel balls lubricated with castor grease, along with the wt% and at% of individual element over a worn surface are depicted in **Figure 5.11a–b**. As shown in **Figure 5.11b**, the signature of carbon on the worn surface was found to be 19.21 wt% which is attributed to the constituents of castor oil–based fatty acids and thickener. Further, the presence of any other foreign particles or additives on the worn surface lubricated with castor grease is ruled out. The signature of oxygen was ascribed due to the formation of oxide film over the worn surface of steel balls. The EDS spectra of steel balls lubricated with 0.02 wt% MoS_2–doped and 0.01 wt% MoS_2–ODT–doped castor

grease, along with the wt% and at% of individual element over a worn surface is shown in **Figure 5.11c–f**. The EDS spectra revealed the presence of nanoadditives constituents on the worn surfaces. The traces of Mo and S confirmed the accumulation/deposition of MoS_2–based nanosheets on the tribo–contacts. Further, the elemental mapping affirmed the uniform distribution of nanoadditives constituents on the interacting surfaces.
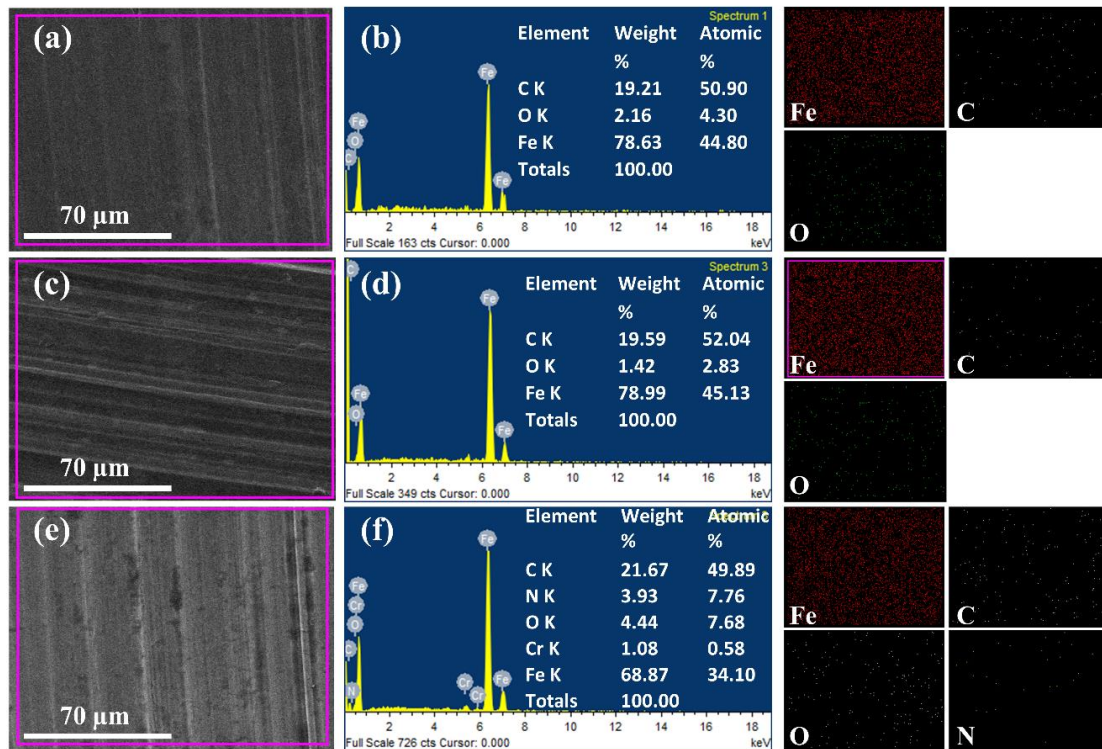

Figure 5.12: EDS spectra with elemental mapping of corresponding worn surfaces of (a–b) 0.05 wt% GO nanosheets in grease (c–d) 0.01 wt% rGO nanosheets in grease (e–f) 0.04 wt% GO–ODA nanosheets in grease. (Applied load: 392 N, test duration: 60 min)

The EDS spectra of worn surface lubricated with graphene–based nanosheets blended castor grease is displayed in **Figure 5.12a–f**. As shown in **Figure 5.12b,d,f**, the signature of carbon was found higher on the worn surface lubricated with graphene–based nanosheets blended castor grease than the worn surface lubricated with castor grease (**Figure 5.11b**). It signified the accumulation/deposition of graphene–based tribo–film on the tribo–contacts. A signature peak of nitrogen besides the iron, carbon, and oxygen was observed

in the EDS spectrum of worn surface lubricated with GO–ODA castor grease (**Figure 5.12f**). The peak of nitrogen is deduced due to nitrogen–constituted ODA. The uniform distribution of all constituent elements of graphene–based nanosheets revealed the formation of good quality of uniform tribo–film, which protects the tribo–contacts against the severe effect of friction and wear.

5.5   Discussion

The lubricants are applied between interacting surfaces to minimize friction and wear. In greases, the beneficial lubrication effect depends critically on base oil viscosity, thickener type and structure, working temperature, surface roughness, and some extent on additives and fillers in the greases (Vengudusamy et al., 2016). The film formation via greases is significantly different and complex from that of oil due to the involvement of thickener. The elastohydrodynamic lubrication (EHL) theory for oil lubrication is well established and conventionally used for grease lubrication. When grease is subjected to continuous shear, the grease will undergo shear degradation and discharge the lube oil to lubricate the interacting surfaces. Herein, the vegetable oil–based greases were formulated with castor oil as a base oil and 12–lithium hydroxystearate metallic soap as a thickener.

The castor oil is obtained from castor seeds which contain ~80% ricinoleic acid as the main content (Zainal et al., 2018). The castor oil has better high–temperature lubrication properties and low–temperature viscosity compared to most vegetable oils (Ogunniyi, 2006). The fatty acids are prime constituents of triglyceride ester of vegetable oil. They contain polar carboxyl group (–COOH), which has an excellent affinity towards metallic surfaces and is believed to facilitate the strong adherence over the steel surfaces under the tribo–stress (Fox and Stachowiak, 2007). The alkyl chains of fatty acids furnish the oleophilicity to engineering surfaces and provide the organized thin film of low shear

strength. The degree of orderness in such thin films is increased with the alkyl chain length.

However, unsaturation destroys the organized structure of fatty acids derived from the thin

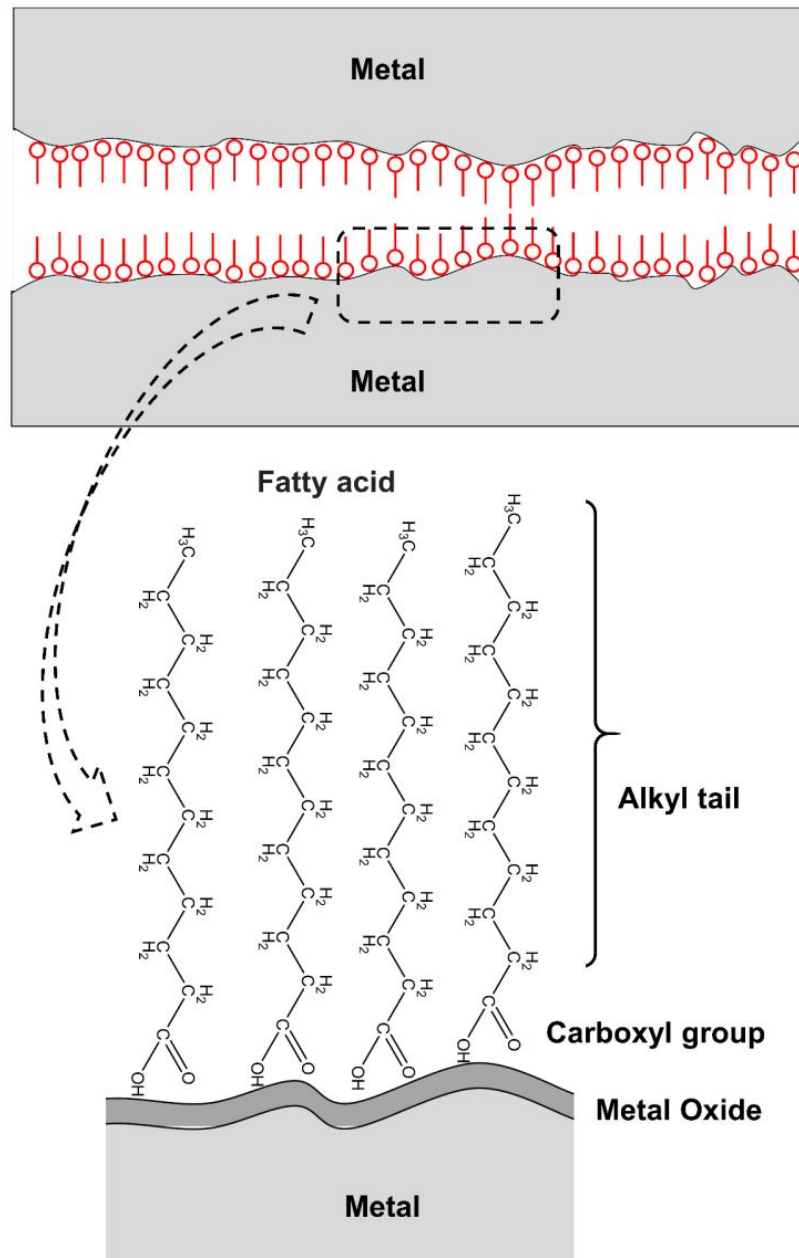film over the steel surface (Sahoo and Biswas, 2009).

Figure 5.13: Plausible interaction between the fatty acids of castor grease and contact interfaces of steel balls. The fatty acids molecules formed the organized thin film over the steel surfaces, driven by tribo–stress

Figure 5.13 demonstrates the plausible structure of fatty acids adsorbed over the steel

surface driven by interaction via the polar carboxylic group. The castor oil is a

monounsaturated fatty acid, which is oriented in organized fashions over the steel surface in a tilted structure driven by weak van der Waals interaction between the alkyl chains of fatty acids and yielded the protective layer of low shear strength (Zachariah et al., 2020). The tribological performance of castor grease was significantly improved in the presence of graphene–based nanoadditives. The use of the 0.5% mass fraction of graphene as an additive in castor oil has reduced the average torque required in the tapping of ADC12 aluminum alloy than pure castor oil (Ni et al., 2018). Similarly, a biodegradable lubricant (a mixture of 40% cashew nut shell liquid and neat castor oil) blended with 0.5% rGO nanoparticles; the tribological performance was enhanced by 61.7% compared to commercial mineral oil (Bhaumik et al., 2021).

The shear degradation of grease discharges the base oil along with nanoadditives. The nanoadditives play a crucial role in boosting the tribological performance of the grease. Herein MoS_2, MoS_2–ODT, GO, rGO, GO–ODA nanosheets in variable dosage (0.01–0.05 wt%) were used as nanoadditives in castor grease. The molecular lamellas of 2D nanoadditives are connected with each other via weak van der Waals interactions. The nanoadditives of layered morphology easily enter into the interface of the tribo–pairs, and the sliding motion of the surfaces forces them to be delaminated and adsorbed on the interacting surfaces and formed a protective tribo–film. The protective transfer film reduces the COF by minimizing the direct interactions of asperities. In the presence of MoS_2–based and graphene–based nanoadditives COF was significantly decreased, which suggests that MoS_2–based and graphene–based nanoadditives have promising potential as AF additive for castor grease. The addition of graphene–based nanoadditives in castor grease exhibited a positive AW effect. It suggests that graphene–based nanoadditives have promising potential as AW additive for castor grease for the given concentration range. On the other hand, MoS_2–based nanoadditives showed a negative AW effect. Guimarey et al. (2020)

have been obtained a reduction in friction and an increment in wear for the lower mass fraction of MoS_2 nanoplatelets, and after 0.1 wt% MoS_2 nanoplatelets improved performance was recorded. Similarly, a reduction in friction and increment in wear for castor grease was obtained due to the low concentration of MoS_2 nanosheets. It suggests that for the given concentration range, MoS_2–based nanoadditives is not compatible for castor grease as AW additive, but it is compatible as AF additive for castor grease.

The interlamellar spacing of nanosheets has a significant effect on the tribological performance of lubricants. Xiao et al. (2015) have examined amine–intercalated α–zirconium phosphate with different interlamellar spaces as a lubricant additive to mineral oil. This study revealed that the maximum friction reduction was accomplished by smaller interlamellar spacing α–zirconium phosphate nanosheets. Similarly, the maximum reduction in friction was achieved by rGO nanosheets having an interlamellar spacing of 0.35 nm between adjacent atomic thick lamella compared to GO nanosheets (0.81 nm). This reduction in the interlamellar spacing of rGO nanosheets was obtained due to the removal of oxygen functionalities and refurbished the characteristic interlayer distance of graphene (Choudhary et al., 2012; Mungse and Khatri, 2014; G. Wang et al., 2008).

5.6   Summary of the chapter

The grease was formulated with castor oil as base oil, and the 12–lithium hydroxystearate was used as a thickener. Further, MoS_2, MoS_2–ODT, GO, rGO, and GO–ODA nanosheets were used as nanoadditives and blended in castor grease in variable concentrations separately. The tribological performance of castor grease with and without nanoadditives was evaluated using a four–ball tester. The experimental results revealed that castor grease in the presence of rGO nanosheets performed superior among all castor grease samples.